Journal of Physiology (1991), **435**, *pp.* 187–205
With 10 figures
Printed in Great Britain

DEPOLARIZATION-MEDIATED INTRACELLULAR CALCIUM TRANSIENTS IN ISOLATED SMOOTH MUSCLE CELLS OF GUINEA-PIG URINARY BLADDER

BY V. YA. GANITKEVICH AND G. ISENBERG

From the Department of Applied Physiology, University of Cologne, D-5000 Köln 41, Germany

(*Received 2 July 1990*)

SUMMARY

1. Free intracellular calcium concentration($[Ca^{2+}]_i$) was recorded in single smooth muscle cells of the guinea-pig urinary bladder held under voltage clamp at 36 °C and 3·6 mM-extracellular Ca^{2+}. The Ca^{2+} indicator Indo-1 was loaded into the cells through patch electrodes. To separate Ca^{2+} currents (I_{Ca}), superimposed K^+ currents were suppressed with a Cs^+ -containing electrode solution.

2. At a holding potential of −60 mV, resting $[Ca^{2+}]_i$ was 114 ± 22 nM (mean ± S.D.). During 160 ms depolarization steps to 0 mV, $[Ca^{2+}]_i$ rose to 885 ± 140 nM. With steps of varied duration, peak $[Ca^{2+}]_i$ increased with the time of depolarization up to about 1 s. Upon repolarization $[Ca^{2+}]_i$ recovered to resting levels with a half-decay time of about 1 s; recovery was not significantly changed with repolarization potentials between −50 and −100 mV.

3. The potential dependence of the above peak $[Ca^{2+}]_i$ transients was bell shaped, with a threshold around −40 mV and a maximum at 0 mV. During depolarization steps to potentials more positive than +80 mV $[Ca^{2+}]_i$ did not significantly rise.

4. During step depolarizations to 0 mV lasting 10 s or longer, $[Ca^{2+}]_i$ peaked within 814 ± 18 ms and then decayed to a sustained level of 250 ± 60 nM. The amplitude of the $[Ca^{2+}]_i$ peak as well as the time course of the transient depended on the amplitude of I_{Ca}. The depolarizations increased $[Ca^{2+}]_i$ to a sustained level with no clearly defined peak when I_{Ca} was reduced by partial inactivation or during steps close to the threshold of I_{Ca} (−40 mV).

5. The sustained level of $[Ca^{2+}]_i$ with longer depolarizations of several seconds showed a bell-shaped voltage dependence with a maximum close to 0 mV. A bell-shaped voltage dependence for $[Ca^{2+}]_i$ was also found during ramp-like depolarizations. However, when the rate of depolarization was low (7·5 mV s^{-1}), the peak $[Ca^{2+}]_i$ was found at more negative potentials (−15 mV).

6. The results are compatible with the idea that Ca^{2+} influx through voltage-operated Ca^{2+} channels is the key event in depolarization-mediated changes in $[Ca^{2+}]_i$ in smooth muscle cells from urinary bladder.

MS 8618

INTRODUCTION

The increase of intracellular free calcium concentration ($[Ca^{2+}]_i$) is a crucial step in the activation of contraction. In smooth muscle, the rise $[Ca^{2+}]_i$ is due to influx from the extracellular space and/or release from intracellular stores. Influx of extracellular Ca^{2+} ions can occur via voltage-dependent calcium channels or through receptor-operated non-selective cationic channels (Benham, 1989*b*). In visceral smooth muscle cells, the Ca^{2+} channels are mainly of the L-type. L-Type Ca^{2+} channels are not gated exclusively by membrane potential, but are characterized by an additional Ca^{2+}-mediated inactivation which constitutes a negative feedback: Ca^{2+} influx elevates $[Ca^{2+}]_i$ and inhibits further Ca^{2+} influx.

These complex voltage- and $[Ca^{2+}]_i$-dependent processes occur when smooth muscles are depolarized (e.g. by excess of extracellular K^+ ions). Since the resulting 'tonic' contracture can be abolished by Ca^{2+} removal from the bath or by Ca^{2+} channel blockers, a sustained Ca^{2+} influx through non-inactivating Ca^{2+} channels has been suggested to be the underlying mechanism (Bolton, 1979; Shuba, 1981). Initial measurements with aequorin demonstrated a sustained ('tonic') elevation of $[Ca^{2+}]_i$ in depolarized preparations (Morgan & Morgan, 1982). However, a quantitative relation between membrane potential and $[Ca^{2+}]_i$ is not available.

The introduction of fluorescent Ca^{2+} probes (Grynkiewicz, Poenie & Tsien, 1985) has resulted in a better understanding of the processes linking depolarization, Ca^{2+} influx, the rise in $[Ca^{2+}]_i$ and the activation of contraction of smooth muscle (Himpens & Somlyo, 1988; Yagi, Becker & Fay, 1988; Becker, Singer, Walsh & Fay, 1989). Applying microspectrofluometry under voltage-clamp conditions allows the pathways for Ca^{2+} influx to be quantified, e.g. non-selective cation channels activated by purinergic receptors (Benham, 1989*b*), Ca^{2+} channels activated by depolarization (Becker *et al.* 1989), and in smooth muscle cells from ureter, the Na^+–Ca^{2+} exchanger (Aaronson & Benham, 1989).

In this study we have investigated changes in $[Ca^{2+}]_i$ in response to depolarization of the surface membrane of voltage-clamped isolated smooth muscle cells. The experiments were performed at 36 °C and 3·6 mM-extracellular calcium to facilitate extrapolation to the *in vivo* situation. The preparation (urinary bladder of the guinea-pig) was chosen because it is electrically excitable, suggesting that I_{Ca} is important for activation of contraction (Creed, 1971). Also, I_{Ca} has been described in these cells (Klöckner & Isenberg, 1985*b*). Finally, the cells are relatively large (diameter about 10 μm) which allows small changes in $[Ca^{2+}]_i$ to be resolved with moderate Indo-1 concentrations (0·1 mM). The results, which describe both transient and sustained changes in $[Ca^{2+}]_i$ in response to depolarization of cell membrane, support the view that Ca^{2+} influx through voltage-operated Ca^{2+} channels is the key event in depolarization-mediated changes in $[Ca^{2+}]_i$.

METHODS

Cell preparation and solutions. Male guinea-pigs were killed by cervical dislocation and single smooth muscle cells were enzymatically isolated according to Klöckner & Isenberg (1985*a*). The cells were continuously superfused with an extracellular solution that contained (in mM): NaCl, 150; $CaCl_2$, 3·6; $MgCl_2$, 1·2; KCl, 5·4; glucose, 20; HEPES, 5; adjusted to pH 7·2 with NaOH. The

pipette solution was composed of (in mM): CsCl, 130; Na_2ATP, 2; $MgCl_2$, 4; HEPES, 5; adjusted to pH 7·2 with approximately 4 mM-NaOH. Thus, the sodium concentration in the pipette solution was about 8 mM. Before each experiment, 0·1 mM of the sodium salt of Indo-1 was added to the pipette solution. The concentration of 0·1 mM was found to be a suitable compromise for measuring fluorescent signals with a reasonable signal-to-noise ratio without buffering the $[Ca^{2+}]_i$ transients too much (Benham, 1989*a*; Neher, 1989). Other calcium buffers were not added to the pipette solution. All experiments were performed at 36 °C. The temperature was controlled by heating device located at the microscope stage close to the chamber.

Voltage clamp. Whole-cell membrane currents were recorded with patch pipettes of 2–4 MΩ resistance. Electrodes were connected to a RK-300 patch-clamp amplifier (Biologic, Echirolles, France). The currents were filtered at 1 kHz and recorded with a Brush pen-writer (Gould Inc., Cleveland, OH, USA; frequency response 50 Hz). The currents were not corrected for leakage. An IBM-compatible microcomputer in combination with a CED-1401 interface (Science Park, Cambridge) was used for generating the voltage-clamp commands and for storing the digitized data.

Fluorescent measurements. For microfluospecroscopy of $[Ca^{2+}]_i$, Indo-1 fluorescence was induced with a single excitation wavelength and dual emission(Grynkiewicz *et al.* 1985; Benham, 1989*a*). A drop of cell suspension was placed in the chamber mounted on the stage of an epifluorescent microscope (Zeiss IM-35) supplemented with a shutter for interrupting the excitation light (75 W xenon lamp). By means of an aperture underneath the objective (Nikon, 100-fold oil immersion), only a part of the cell (about 30 μm diameter) was illuminated at 340 nm. The light emitted from this region was split by dichroic mirrors. Thus, the light was collected from about one-fifth of the cell which was typically 150–200 μm long. Photons in the bands between 395 and 425 nm and 450 and 490 nm were collected by a pair of photomultipliers (Hamamatsu Photonics, Japan) and amplifiers (Dr Seitner, Seewiesen, Germany). After filtering at 20 or 50 Hz, an analog divider (Burr Brown DIV100) delivered the fluorescence ratio 410/470 on line. At both wavelengths, the background fluorescence was subtracted electronically when the pipette (containing Indo-1) was attached to a part of the cell that was masked by the aperture. After the whole-cell configuration was achieved by rupture of the membrane patch, at least 5 min of loading with Cs^+ and Indo-1 were allowed before the experiment was started. During the loading period, the cells were neither stimulated nor illuminated.

Calibration of $[Ca^{2+}]_i$. The relationship between $[Ca^{2+}]_i$ and the recorded ratio of signals 410/470 (R) is given by an equation (Grynkiewicz *et al.* 1985)

$$[Ca^{2+}]_i = K_d B(R-R_{min})/(R_{max}-R),$$

where K_d is the effective dissociation constant of Indo-1, B is F_o/F_s, i.e. the ratio of fluorescent signals at 470 nm without Ca^{2+} (F_o) and with saturating Ca^{2+} (F_s). R_{min} is the 410/470 ratio in the absence of Ca^{2+}, and R_{max} is the 410/470 ratio at saturating calcium concentration. Since the properties of Indo-1 seem to be different in the cell as compared to aqueous solutions (Almers & Neher, 1985), an intracellular calibration procedure was used (Almers & Neher, 1985; Benham, 1989*a*; Neher, 1989). At the end of each experiment the cell membrane was made leaky by stepping to −200 or −400 mV (Benham, 1989*a*). This resulted in a large increase in R within 1–2 min. R continued to increase, probably due to the large current flow through the leaky membrane into the pipette, corresponding to an ionophoresis of calcium ions into the pipette. The slow increase was prevented by stepping the membrane potential to 0 mV. R_{max} was taken to be the value reached by R in a leaky cell at 0 mV at the end of each experiment. Typically, R_{max} was between 0·4 and 0·5.

R_{min} was measured in cells perfused with a solution containing 10 mM-EGTA (Neher, 1989). For comparison, R_{min} was also measured with pipette solution containing 40 mM-EGTA and 10 mM-BAPTA. These values were not significantly different. For example, the mean value of R_{min} with 10 mM-EGTA was 0·094; with 40 mM-EGTA and 10 mM-BAPTA it was 0·090. The quantity K_dB was estimated by perfusing the cell with a solution containing Ca^{2+}-EGTA buffer (see Benham, 1989*a*; Neher, 1989). At pH 7·2, a solution containing 6 mM-Ca^{2+}-EGTA and 3 mM-free EGTA was assumed to contain 309 nM-free Ca^{2+} (Benham, 1989*a*; Neher, 1989). A period of 5 min was sufficient to eliminate the depolarization-mediated changes in the 410/470 ratio suggesting adequate buffering of intracellular calcium. From the measured value R_{309}, the K_dB value of 862 nM was evaluated.

Reliability of calibration procedure. Although the intracellular calibration procedure seems to be quite adequate (Neher, 1989), there are still many places for errors. This probably accounts for the scattering in $[Ca^{2+}]_i$ measured between different cells. For example, resting $[Ca^{2+}]_i$ was between 80 and 170 nM while peak $[Ca^{2+}]_i$ was between 400 and 1100 nM despite comparable values of I_{Ca}. Nevertheless, the method used provides a sensitive tool for measuring changes in $[Ca^{2+}]_i$ which was the object of the present study. Where appropriate, the results are presented as means ± S.D. Otherwise the traces represent typical results from at least four similar experiments.

RESULTS

$[Ca^{2+}]_i$ *transients in response to 160 ms depolarization steps to 0 mV*

In thirty-two cells, held under voltage clamp at −60 mV, the resting calcium concentration $[Ca^{2+}]_i$ was 114 ± 22 nM (individual values between 80 and 170 nM). $[Ca^{2+}]_i$ did not change significantly during diffusion of Indo-1 from the patch pipette into the cell, suggesting that the Ca^{2+}-buffering capacity was not significantly increased. This assumption is also supported by the result that the activity of spontaneous transient outward currents (STOCs), recorded with KCl electrodes at a clamp potential of −40 or −30 mV, was not suppressed by the loading of Indo-1. It was possible to resolve small changes in $[Ca^{2+}]_i$ during the appearance of STOCs. However, no attempt was made to correlate these since STOCs seem to represent local events in whole-cell current recordings while the light was collected only from the part of the cell.

Depolarization steps to 0 mV evoked inward calcium currents (I_{Ca}) and caused a simultaneous rise in $[Ca^{2+}]_i$ (Fig. 1, left traces). $[Ca^{2+}]_i$ always peaked at the end of the 160 ms pulse. On average, peak $[Ca^{2+}]_i$ was 885 ± 140 nM ($n = 20$, values between 400 and 1100 nM). At the beginning of depolarization, when the amplitude of I_{Ca} was large, $[Ca^{2+}]_i$ rose with an initial high rate (9 μM s^{-1}). Later, at the end of depolarization, when the I_{Ca} was partially inactivated, the rate of rise decreased to 2 μM s^{-1}. The rate of rise in $[Ca^{2+}]_i$ corresponded to the instantaneous amplitude of I_{Ca}, so that the time course of the $[Ca^{2+}]_i$ transient and the time integral of I_{Ca}, were similar (compare Becker *et al.* 1989). This result suggests that Ca^{2+} influx through voltage-operated Ca^{2+} channels is closely linked to the depolarization-mediated increase in $[Ca^{2+}]_i$.

Upon repolarization to −60 mV, $[Ca^{2+}]_i$ slowly recovered to resting levels. Recovery was completed within 4–6 seconds (Fig. 1, left traces) at a rate of about 0·2 μM s^{-1}, or about 40 times slower than the maximal rate of rise of $[Ca^{2+}]_i$. The recovery of $[Ca^{2+}]_i$ could not be fitted to a single exponential. Therefore, it was described with a half-decay time of about 1 s. Due to the slow time course of the recovery phase, the effect of individual depolarizing clamp steps could be summed. Figure 1 (middle traces) shows changes in $[Ca^{2+}]_i$ resulting from a pair of pulses. During the first pulse $[Ca^{2+}]_i$ peaked to 800 nM. Following 200 ms repolarization to −60 mV, $[Ca^{2+}]_i$ decayed to 700 nM. The second pulse induced a smaller $[Ca^{2+}]_i$ transient that started from 700 nM and peaked at 1100 nM (i.e. 400 nM). Reduction of the second $[Ca^{2+}]_i$ transient could be attributed to the reduction of I_{Ca}. However, I_{Ca} was reduced by only 25%, suggesting that other processes may be involved. For example, contribution of Ca^{2+} released from intracellular stores could be larger during the first pulse, when the stores are filled, than during the second pulse, when they have been deprived of releasable Ca^{2+}.

Upon repetitive stimulation with trains of voltage steps, the individual $[Ca^{2+}]_i$ transients superimposed to form a 'tetanic' response (Fig. 1, right traces). At a frequency of 1 Hz, the 840 ms repolarization period between the pulses was insufficient for the recovery of $[Ca^{2+}]_i$ to resting values. Due to this, $[Ca^{2+}]_i$ fluctuated between

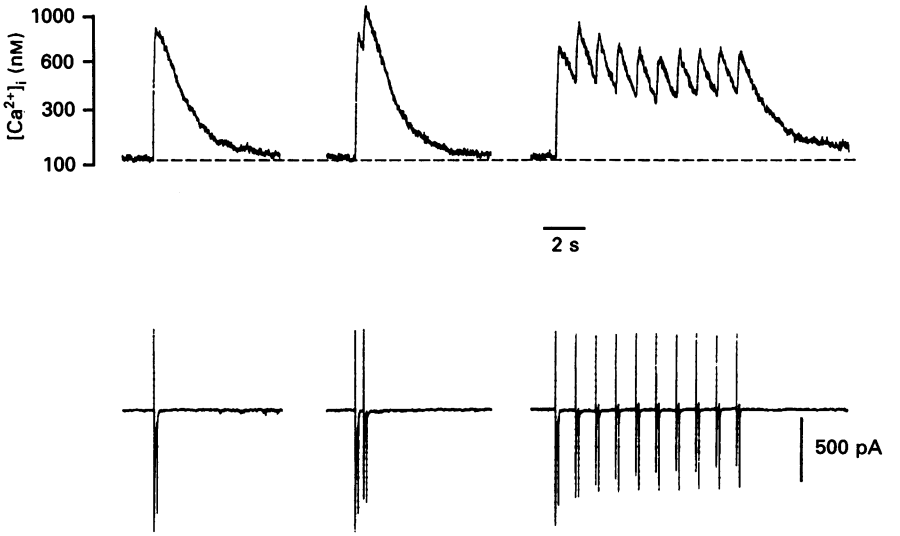

Fig. 1. Membrane currents in response to 160 ms step depolarizations to 0 mV from holding potential of −60 mV and associated changes in $[Ca^{2+}]_i$. $[Ca^{2+}]_i$ transients are shown in response to a single pulse (left), a pair of pulses separated by a 200 ms interval (middle), and a train of 10 pulses at 1 Hz frequency (right). Note that in this and following figures the scaling of $[Ca^{2+}]_i$ is not linear.

350 and 700 nM. However, the tetanic response was not a real summation: peak $[Ca^{2+}]_i$ obtained during pulses 3 to 10 did not exceed the peak $[Ca^{2+}]_i$ of the first pulse. I_{Ca} displayed a negative staircase effect since interpulse interval was not sufficient for recovery of I_{Ca} from inactivation.

During the 160 ms depolarization, I_{Ca} did not completely inactivate. Repolarization to −70 mV increased the driving force for Ca^{2+} ions, and Ca^{2+} influx through rapidly deactivating calcium channels occurred (tail current). At −60 or −70 mV, the tail current did not visibly increase $[Ca^{2+}]_i$. Instead there was an immediate transition to the slow recovery phase upon repolarization (Fig. 2*A*; see also Aaronson & Benham, 1989).

I_{Ca} tail currents did induce calcium transients, however, when a different pulse protocol was applied. In the experiment of Fig. 2*B*, Ca^{2+} channels were activated by a 160 ms step to +90 mV. (During this depolarization, the rise in $[Ca^{2+}]_i$ was nearly negligible.) The voltage step from +90 to 0 mV induced a large I_{Ca} tail current (marked by arrow in Fig. 2*B*) and a rise in $[Ca^{2+}]_i$ that started at a high rate and peaked after about 750 ms. The 'tail transients' were not observed when the membrane was repolarized from +90 mV to potentials more negative than −40 mV (Fig. 3*A*).

Voltage-dependent $[Ca^{2+}]_i$ transients elicited by 160 ms pulse depolarizations

Information about the voltage dependence of the $[Ca^{2+}]_i$ is critical for distinguishing between mechanisms underlying $[Ca^{2+}]_i$ transients: Ca^{2+} influx through channels, through the Na^+–Ca^{2+} exchanger, Ca^{2+} release from intracellular

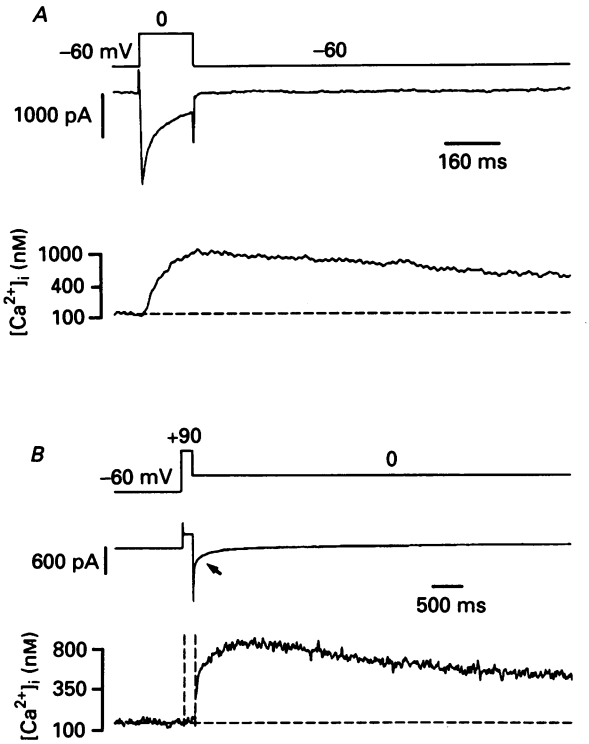

Fig. 2. $[Ca^{2+}]_i$ transients in response to depolarization (*A*) and repolarization (*B*) of the membrane. *A*, calcium current (middle trace) and $[Ca^{2+}]_i$ transient (lower trace) during 160 ms depolarization from −60 to 0 mV. Voltage protocol is shown in the upper trace. *B*, membrane current (middle trace) and associated $[Ca^{2+}]_i$ transient (lower trace). Membrane potential was stepped for 160 ms from −60 to +90 mV and then to 0 mV. Pulse protocol is shown in upper trace. I_{Ca} tail current is indicated by arrow. *A* and *B* from different cells.

stores, triggered by either Ca^{2+} or depolarization. Figure 2 has already shown that the strong depolarization to +90 mV failed to change $[Ca^{2+}]_i$. The complete voltage dependence of the $[Ca^{2+}]_i$ transients is presented in Fig. 3. When starting from holding potential of −60 or −70 mV, depolarizations to a threshold potential of −40 mV were required for the first measurable changes in $[Ca^{2+}]_i$ (Fig. 3*A*). With more positive potential steps, the amplitude of the $[Ca^{2+}]_i$ transients increased. $[Ca^{2+}]_i$ transients of maximal amplitude were usually found at 0 mV. Steps to more and more positive potentials induced $[Ca^{2+}]_i$ transients of progressively smaller amplitude. Finally, steps to membrane potentials of +80 or +100 mV had no affect on $[Ca^{2+}]_i$.

The voltage dependence of the $[Ca^{2+}]_i$ transient measured in this way was bell shaped (Fig. 3*B*, ●). It resembles the bell-shaped voltage dependence of peak I_{Ca} (Fig. 3*B*, ○). Between −40 and +30 mV, the curves resemble each other. At more positive potentials, however, I_{Ca} reverses polarity whereas the $[Ca^{2+}]_i$ transient

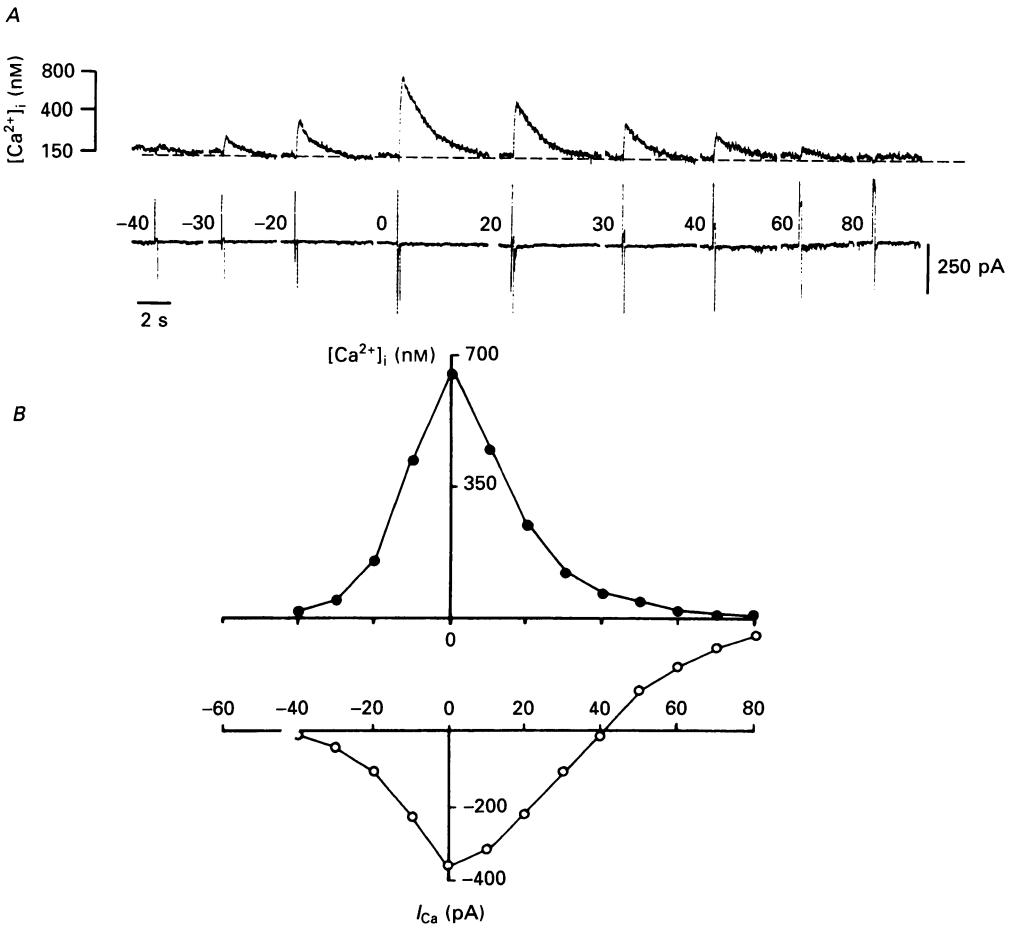

Fig. 3. Potential dependence of $[Ca^{2+}]_i$ transients during 160 ms step membrane depolarizations from the holding potential of −60 mV. *A*, traces of $[Ca^{2+}]_i$ (upper trace) and membrane current (lower trace). Frequency of depolarizing pulses was 0·1 Hz. *B*, plot of changes if $[Ca^{2+}]_i$ (●) and peak calcium current (○) *versus* potential of step depolarization. *A* and *B* from the same cell.

asymptotically approaches zero. This result is in line with a model of ion permeation through calcium channels (Hess & Tsien, 1984) which predicts that at potentials positive to +40 mV, Cs^+ efflux through calcium channels exceeds Ca^{2+} influx, resulting in a net outward current.

Effect of duration of depolarization steps to 0 mv on the $[Ca^{2+}]_i$ *transient*

Repolarization to −60 mV abbreviated the depolarization-mediated increase in $[Ca^{2+}]_i$ (Figs 2*A* and 4*A*, middle panel). When the depolarization was restricted to 16 ms, the rise in $[Ca^{2+}]_i$ was brief and the peak was correspondingly small (Fig. 4*A*, left-hand panel). Peak $[Ca^{2+}]_i$ increased with length of the depolarizing step.

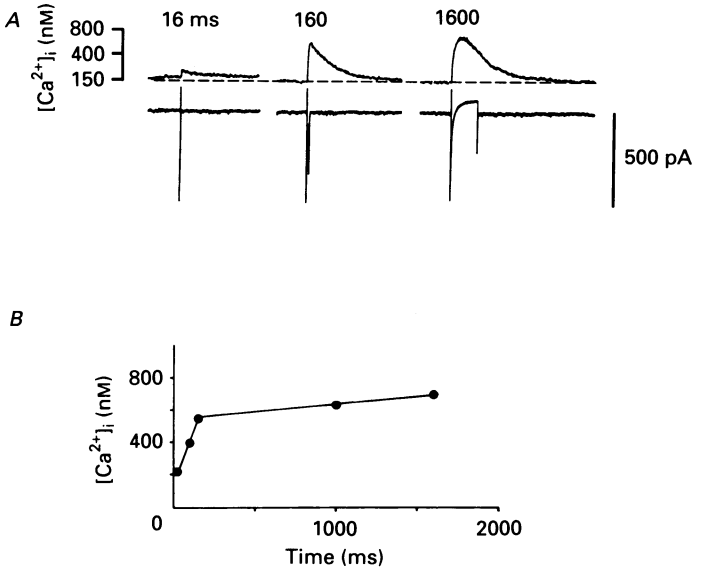

Fig. 4. Dependence of $[Ca^{2+}]_i$ transients on the duration of depolarizing pulse. *A*, $[Ca^{2+}]_i$ transients (upper trace) and membrane currents (lower trace) are shown in response to step depolarizations from −60 to 0 mV when the duration of the pulse was 16 ms (left), 160 ms (middle) and 1·6 s (right). *B*, dependence of peak $[Ca^{2+}]_i$ on the duration of depolarizing pulse.

However, during depolarizations longer than 1 s, $[Ca^{2+}]_i$ peaked before the end of depolarization (right-hand panel in Fig. 4*A*). On average, this peak $[Ca^{2+}]_i$ was reached 814 ± 18 ms after the step to 0 mV ($n = 17$). The peak of $[Ca^{2+}]_i$ during a sustained depolarization was the reason that the duration dependence of peak $[Ca^{2+}]_i$ showed saturation for long pulses (Fig. 4*B*). This saturation differs from the continuous rise in $[Ca^{2+}]_i$ up to 10 s at depolarizations to 0 mV reported for guinea-pig ureter myocytes or pituitary cells (Aaronson & Benham, 1989; Benham, 1989*a*).

$[Ca^{2+}]_i$ *changes during long-lasting depolarizations*

When depolarization was continued, after reaching the peak, $[Ca^{2+}]_i$ fell to a level higher than resting. $[Ca^{2+}]_i$ remained at this sustained elevated level as long as the membrane was depolarized. During a 20 s depolarization to 0 mV, for instance, $[Ca^{2+}]_i$ peaked within 830 ms to 870 nM and then slowly fell within 10 s to a sustained level of 270 nM. During repolarization of the membrane to −70 mV, $[Ca^{2+}]_i$ fell to the resting level within 4 s. Both peak and sustained elevations of $[Ca^{2+}]_i$ were abolished

by calcium removal from the bath or by bath application of 1 mM-Cd^{2+}, suggesting that they require calcium influx from the extracellular space.

The time course of the $[Ca^{2+}]_i$ transient as well as the values of peak and sustained $[Ca^{2+}]_i$ depended on the holding potential and the potential of the step depolarization.

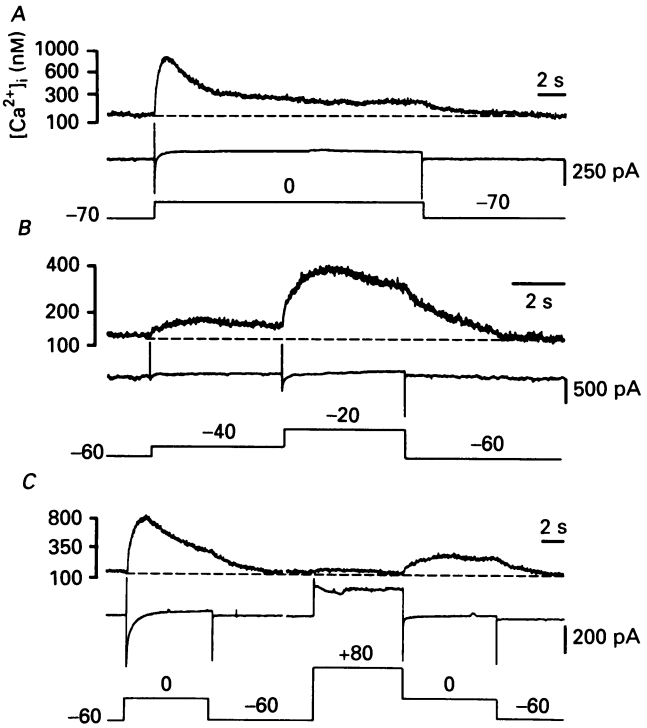

Fig. 5. $[Ca^{2+}]_i$ transients during long-lasting depolarizations of the membrane. *A*, membrane potential was stepped from −70 to 0 mV (voltage protocol, lower trace). Membrane current (middle trace) and corresponding $[Ca^{2+}]_i$ transient (upper trace) are shown. *B*, membrane potential was stepped from −60 to −40 mV and then to −20 mV (lower trace). Middle and upper traces show membrane current and $[Ca^{2+}]_i$ transient, respectively. *C*, effect of conditioning step to +80 mV on the $[Ca^{2+}]_i$ transient (upper trace) at 0 mV. Membrane current is shown in middle trace. Lower trace shows voltage-clamp protocol (in mV). *A*, *B* and *C* from different cells.

During depolarizations to −40 mV (close to the threshold of I_{Ca}), $[Ca^{2+}]_i$ increased at a slow rate and a small peak of 180 nM was reached within 2·2 s. Stepping from −40 to −20 mV evoked a partially inactivated I_{Ca}, and $[Ca^{2+}]_i$ increased to 380 nM within 1·9 s. From the peak, $[Ca^{2+}]_i$ decayed to a sustained value higher than the one at −40 mV (Fig. 5*B*). Repolarization to −60 mV resulted in a recovery of $[Ca^{2+}]_i$ to the original resting level. The differences in the $[Ca^{2+}]_i$ transients at −40, −20 and 0 mV illustrate that more positive clamp-step potentials increase both the rate of rise and the rate of decay of the $[Ca^{2+}]_i$ response (Fig. 5*A* and *B*).

Figure 5*C* demonstrates the influence of I_{Ca} inactivation on the time course of the $[Ca^{2+}]_i$ transients at 0 mV. When the step started from −60 mV, it induced an I_{Ca} and an increased $[Ca^{2+}]_i$ which peaked and then decayed towards a sustained level.

When the same cell was held at +80 mV for 8 s and then stepped to 0 mV, only a small and slow rise in $[Ca^{2+}]_i$ without a peak was recorded, i.e. the rapid rise to the peak and the following decay were absent. The response differs from the one of Fig. 2*B* because of the duration of the depolarization to +80 mV. Whereas an I_{Ca} tail

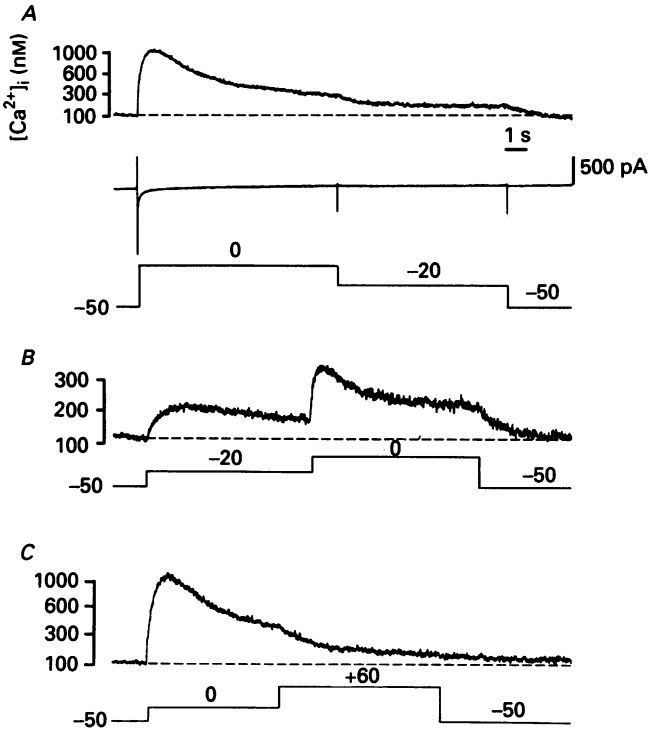

Fig. 6. Potential dependence of sustained level of $[Ca^{2+}]_i$ studied using step changes in membrane potential. *A*, membrane potential was stepped from −50 to 0 mV and then to −20 mV (lower trace). Corresponding membrane current is shown in the middle trace and $[Ca^{2+}]_i$ transient in the upper trace. *B*, membrane potential was stepped from −50 to −20 mV and then to 0 mV (lower trace). Corresponding changes in $[Ca^{2+}]_i$ are shown in the upper trace. *C*, clamp potential was changed from −50 to 0 mV and then to +60 mV (lower trace). $[Ca^{2+}]_i$ transient shown in upper trace. *A*, *B* and *C* from different cells.

current and a rapid rise of $[Ca^{2+}]_i$ were recorded after a 160 ms depolarization to +90 mV (Fig. 2*B*), both the tail I_{Ca} and the rapid $[Ca^{2+}]_i$ transient were absent after I_{Ca} was largely inactivated by a 8 s depolarization to +80 mV (Fig. 5*C*). The transient during the potential step from +80 to 0 mV, i.e. the slow increase to a sustained $[Ca^{2+}]_i$, resembled the one recorded with the step from −60 to −40 mV (compare panel *C* to panel *B* in Fig. 5).

Voltage dependence of sustained level of $[Ca^{2+}]_i$

The dependence of sustained $[Ca^{2+}]_i$ on membrane potential was studied by stepping to a new potential after the $[Ca^{2+}]_i$ transient approached a steady state. Figure 6*A*, for example, demonstrates that sustained $[Ca^{2+}]_i$ at 0 mV (300 nM) could be diminished (210 nM) by stepping to a potential 20 mV more negative.

Repolarization to −50 mV induced a complete recovery of $[Ca^{2+}]_i$, and it could not be further reduced by stepping to −60 or −70 mV. Figure 6*B* shows the opposite sequence of voltage steps, i.e. the potential was stepped initially from −50 to −20 and then to 0 mV. Again, the sustained $[Ca^{2+}]_i$ was higher at 0 mV than at −20 mV.

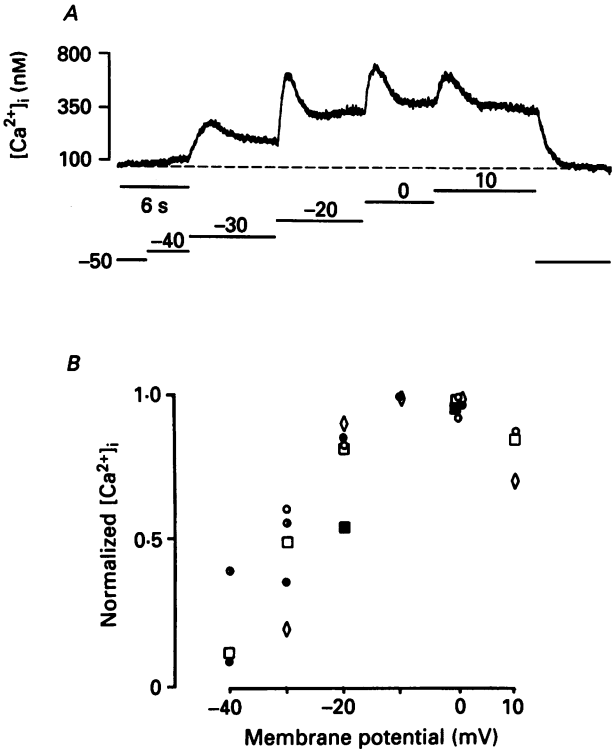

Fig. 7. Sustained level of $[Ca^{2+}]_i$ as a function of membrane potential. *A*, membrane was depolarized from −50 to −40, −30, −20, 0 and +10 mV, consecutively. $[Ca^{2+}]_i$ transient, upper trace; voltage protocol, lower trace. *B*, voltage dependence of normalized sustained level of $[Ca^{2+}]_i$ from six cells. The sustained value reached by $[Ca^{2+}]$ at different potentials was normalized to the maximal value observed in five cells at 0 mV and in one cell at −10 mV.

A significant decrease in sustained $[Ca^{2+}]_i$ was also observed when the membrane potential was stepped from 0 to +60 mV (Fig. 6*C*).

The sustained level of $[Ca^{2+}]_i$ achieved with long-lasting depolarizations did not clearly demonstrate the dependence on the holding membrane potential. Therefore, the voltage dependence of sustained $[Ca^{2+}]_i$ was also studied with potential steps that progressively depolarized the membrane (Fig. 7*A*). Between −50 and 0 mV, the sustained level of $[Ca^{2+}]_i$ progressively increased, whereas at +10 mV the sustained level of $[Ca^{2+}]_i$ was slightly lower than at 0 mV. Data from six cells are summarized in the plot of Fig. 7*B* that reveals a bell-shaped voltage dependence of sustained levels of $[Ca^{2+}]_i$. The threshold was around −40 mV, and the maximum between −10 and 0 mV. Thus, the voltage dependence of sustained levels of $[Ca^{2+}]_i$ resembled the bell-shaped curves described for the 160 ms $[Ca^{2+}]_i$ transient (Fig. 3) and for I_{Ca}.

Voltage dependence of $[Ca^{2+}]_i$ *studied with ramp-like depolarizations*

The bell-shaped voltage dependence of $[Ca^{2+}]_i$ can be demonstrated directly by repolarizing the membrane with ramp-like voltage commands. In order to bring inactivation of I_{Ca} and $[Ca^{2+}]_i$ close to a steady state, the experiments started with

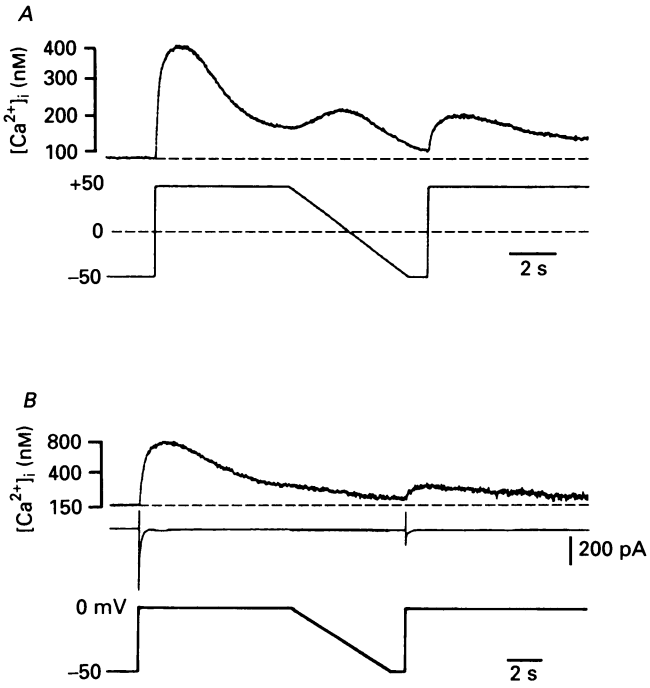

Fig. 8. Potential dependence of sustained level of $[Ca^{2+}]_i$ following ramp changes in membrane potential. *A*, potential was stepped from −50 to +50 mV for 6 s and then at a rate of 20 mV s^{-1}, the membrane was repolarized to −50 mV (lower trace). Corresponding $[Ca^{2+}]_i$ transient is shown in upper trace. *B*, in another cell, the membrane was depolarized from −50 to 0 mV for 8 s and then slowly (10 mV s^{-1}) repolarized to −50 mV (lower trace). Corresponding membrane current and $[Ca^{2+}]_i$ transient are shown in middle and upper traces.

5–8 s long depolarizing steps. When $[Ca^{2+}]_i$ approached a sustained value of 160 nM after depolarization to +50 mV, the membrane was repolarized to −50 mV at a rate of 20 mV s^{-1}. The transient increase in $[Ca^{2+}]_i$ to 220 nM observed during the repolarization occurred at potentials close to 0 mV (Fig. 8*A*). At more negative potentials, $[Ca^{2+}]_i$ fell and at −50 mV it was close to the resting value (100 nM). In conclusion, the voltage dependence of $[Ca^{2+}]_i$ observed with ramp-like repolarizations from +50 mV to −50 mV resembled the bell-shaped voltage dependence that was described for the $[Ca^{2+}]_i$ transient (Fig. 3) and for sustained level of $[Ca^{2+}]_i$ (Figs 6 and 7).

The bell-shaped voltage dependence of $[Ca^{2+}]_i$ (Fig. 8*A*) suggests that, between +50 and 0 mV, the ramp-like repolarization increased the driving force for Ca^{2+} ions faster than the extent of I_{Ca} inactivation. At negative potentials, however, $[Ca^{2+}]_i$

and Ca^{2+} influx are thought to fall because of progressive deactivation of the Ca^{2+} channels. The last effect is seen in the experiment of Fig. 8*B*. When the sustained $[Ca^{2+}]_i$ (300 nM) was almost reached, the membrane was repolarized to −50 mV at a rate of 10 mV s^{-1}. Repolarization resulted in a continuous decrease in $[Ca^{2+}]_i$ towards the resting level.

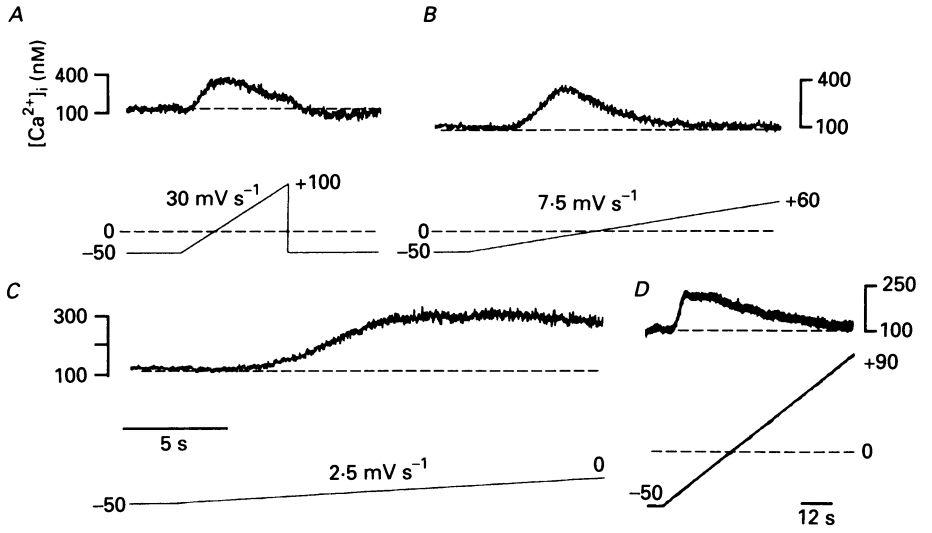

Fig. 9. Effect of rate of rise of membrane depolarization on the $[Ca^{2+}]_i$ transient. The upper traces show the changes in $[Ca^{2+}]_i$, and the lower ones show the voltage protocol. Rate of membrane depolarization was 30 (*A*), 7·5 (*B*) and 2·5 mV s^{-1} (*C* and *D*). *A*, *B*, *C* and *D* were obtained from different cells.

Dependence of $[Ca^{2+}]_i$ transients on the rate of ramp-like depolarizations

The experiments with slowly changing depolarizations are interesting because they can be used as a model for agonist-induced depolarization leading to activation of voltage-dependent Ca^{2+} channels (Bolton, 1979; Shuba, 1981). Due to the time-dependent activation and inactivation of Ca^{2+} channels, it is not only the amplitude but also the rate of the voltage change that determines the number of open Ca^{2+} channels and thereby the amount of Ca^{2+} influx. Figure 9 shows corresponding changes in $[Ca^{2+}]_i$ when the membrane was depolarized from −50 mV with a speed of 30, 7·5 or 2·5 mV s^{-1}.

Figure 9*A* shows the changes in $[Ca^{2+}]_i$ that are induced by depolarization at a relatively high rate (30 mV s^{-1}). Starting from a resting concentration of 120 nM, $[Ca^{2+}]_i$ increased when depolarization reached −30 mV. Continuing depolarization induced a progressive increase in $[Ca^{2+}]_i$ until a maximum $[Ca^{2+}]_i$ (380 nM) was reached at potentials between 0 and +10 mV. At more positive potentials $[Ca^{2+}]_i$ decayed again. When the ramp was terminated at +100 mV, $[Ca^{2+}]_i$ was still above the resting level; probably, during the fast ramp, there was not enough time for recovery of $[Ca^{2+}]_i$.

Figure 9*B* shows the changes in $[Ca^{2+}]_i$ obtained with slower depolarization rate (7·5 mV s^{-1}). In contrast to Fig. 9*A*, maximal $[Ca^{2+}]_i$ was recorded at −15 mV, and

$[Ca^{2+}]_i$ decayed to nearly resting levels at potentials positive to +40 mV. When the rate of depolarization was as slow as 2·5 mV s^{-1} (Fig. 9*C* and *D*), $[Ca^{2+}]_i$ started to rise at −40 mV (Fig. 9*C*). Maximal $[Ca^{2+}]_i$ was reached close to −25 mV. Despite continuing depolarization, $[Ca^{2+}]_i$ remained at this level until the membrane was

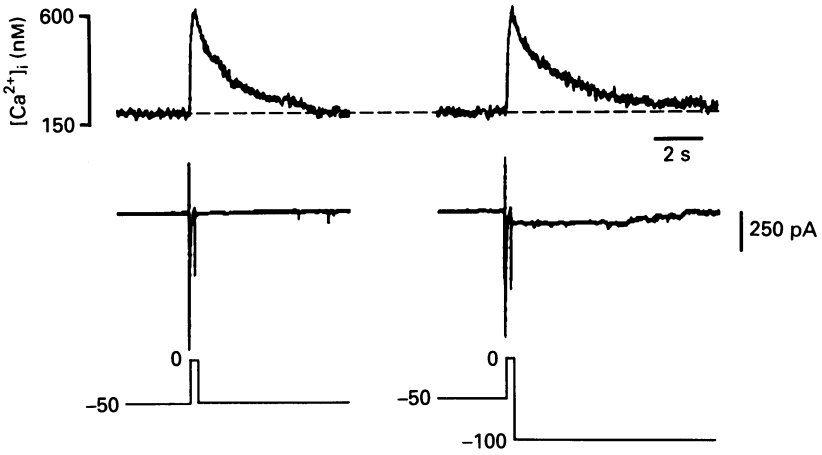

Fig. 10. Effect of membrane potential on decay of the $[Ca^{2+}]_i$ transient. Voltage-clamp protocol is shown in the lower traces, membrane currents and $[Ca^{2+}]_i$ transients in the middle and upper traces, respectively.

depolarized close to −10 mV. At more positive potentials, $[Ca^{2+}]_i$ decayed to the resting value (Fig. 9*D*).

Na^+–Ca^{2+} exchange does not significantly change $[Ca^{2+}]_i$

The comparison of voltage dependencies of $[Ca^{2+}]_i$ and I_{Ca} rules out the possibility of contribution from other voltage-dependent Ca^{2+} fluxes, i.e. the electrogenic Na^+–Ca^{2+} exchange (Beuckelmann & Wier, 1988; Aaronson & Benham, 1989). The lack of any significant contribution of the Na^+–Ca^{2+} exchanger to Ca^{2+} influx has already been indicated by the bell-shaped voltage dependence of $[Ca^{2+}]_i$ (Figs 3, 6 and 8). The results also suggest that Ca^{2+} efflux through the Na^+–Ca^{2+} exchanger is negligible. The rate of Ca^{2+} efflux through the Na^+–Ca^{2+} exchanger has been reported to increase with more negative membrane potentials (Beuckelmann & Wier, 1988). For this reason, we examined the influence of membrane potential on the recovery of $[Ca^{2+}]_i$ to the resting level. Figure 10 shows that $[Ca^{2+}]_i$ transients, evoked by 160 ms pulses from −50 to 0 mV, recovered at −50 mV and at −100 mV along similar time courses, i.e. $[Ca^{2+}]_i$ fell to 50% of the peak value within 0·8 s at −50 mV and within 0·9 s at −100 mV. On average, the half-decay time was 0·90±0·13 s at −50 and 0·92±0·11 s at −100 mV ($n = 4$). The values are not significantly different, suggesting that Ca^{2+} efflux through the electrogenic Na^+–Ca^{2+} exchanger does not significantly contribute in this potential range to the recovery of $[Ca^{2+}]_i$ to the resting level.

DISCUSSION

The results of this paper relate depolarization-mediated changes in $[Ca^{2+}]_i$ to Ca^{2+} influx through potential-dependent Ca^{2+} channels. At holding potentials close to the resting potential (−50 or −60 mV) $[Ca^{2+}]_i$ was 114 nM, an estimate close to the resting $[Ca^{2+}]_i$ of other smooth muscle cells as measured with Indo-1 (Aaronson & Benham, 1989; 130 nM in guinea-pig ureter; Benham, 1989*b*; 140 nM in rabbit ear artery), and with Fura-2 (Yagi *et al.* 1988: 150 nM in toad stomach; Goldman, Wier & Blaustein, 1989: 111 nM in bovine tail artery), or with ion-sensitive electrodes (Yamaguchi, 1986: 160 nM in toad stomach). Small depolarizations induced only small changes in $[Ca^{2+}]_i$, e.g. $[Ca^{2+}]_i$ rose by only 50 nM at −40 mV. For optimal resolution, the fluorescence was excited by the full intensity of the light source with the result that within 2 min significant bleaching of intracellular Indo-1 occurred, thus restricting the time of recordings. In addition, the signals were filtered at 20 or 50 Hz (25 dB), which can result in a delay in the onset and attenuation of rapid peaks. This prevented us from analysing fast events, such as the latency period or the initial maximal rate of rise of $[Ca^{2+}]_i$. Nevertheless, our results show that it is possible to measure depolarization-induced changes in $[Ca^{2+}]_i$ at physiological temperatures (36 °C) and 3·6 mM $[Ca^{2+}]_o$.

The hypothesis, that depolarization controls $[Ca^{2+}]_i$ and contraction via Ca^{2+} influx through Ca^{2+} channels, was tested in experiments where I_{Ca} and $[Ca^{2+}]_i$ were measured simultaneously. Pulses (160 ms) to 0 mV increased $[Ca^{2+}]_i$ to about 900 nM. This peak value is somewhat higher than that reported for similar depolarizations at room temperature in other smooth muscle cells (Aaronson & Benham, 1989: 250 nM; Yagi *et al.* 1988; Becker *et al.* 1989: 400 nM). The difference is most probably due to increase of peak I_{Ca} with temperature.

The increment in $[Ca^{2+}]_i$ during Ca^{2+} influx can be related to the charge transported by I_{Ca}, as calculated from the time integral of I_{Ca}. For the 160 ms pulses the value of about 5 nM pC^{-1} can be evaluated. This number is similar to those reported in other smooth muscle cells (Benham, 1989*b*), neurones (Thayer, Hirning & Miller, 1988), and pituitary cells (Benham, 1989*a*). During the period of the 160 ms pulse, the increment in total intracellular calcium due to Ca^{2+} influx into a cell of 6 pl volume was estimated as 10–20 μM. This number is up to 20 times larger than the observed increase in free calcium (about 1 μM), suggesting that most of the inflowing Ca^{2+} is bound (compare Becker *et al.* 1989). Smooth muscle cells, like other cells, are known to contain a variety of calcium-binding proteins which are thought to bind rapidly most of the calcium ions entering the cell. Obviously, whether Ca^{2+} influx is large enough to cause the observed change in the free calcium depends on the assumptions of the calcium-binding properties of the intracellular proteins. For vascular smooth muscle cells, large amounts of calcium are bound to calmodulin, myosin, F-actin and other proteins (Bond, Shuman, Somlyo & Somlyo, 1984). If similar calcium-binding properties are assumed in smooth muscle cells of urinary bladder, it is quite likely that the peak of the depolarization-mediated increase in $[Ca^{2+}]_i$ results not only from Ca^{2+} influx but also from the release of Ca^{2+} from intracellular stores. The possible contribution of Ca^{2+} release was discussed previously when we described changes in $[Ca^{2+}]_i$ upon depolarization with a pulse pair (Fig. 1).

However, which fraction of the $[Ca^{2+}]_i$ transient is due to influx and which to release cannot be answered by the present results, therefore making quantitative correlation between calcium current density and changes in $[Ca^{2+}]_i$ difficult.

If the depolarization-mediated rise in $[Ca^{2+}]_i$ includes significant contributions from Ca^{2+} release, then in order to explain the bell-shaped voltage dependence, as well as the $[Ca^{2+}]_i$ transient induced by I_{Ca} tail currents (Fig. 2*B*), we should invoke a 'Ca^{2+} -induced release of Ca^{2+}' as in heart muscle (Fabiato, 1983; Beuckelmann & Wier, 1988) and not a 'depolarization-induced release of Ca^{2+}' as in skeletal muscle (Melzer, Schneider, Simon & Szucs, 1986). These results illustrate that analysis of $[Ca^{2+}]_i$ under voltage-clamp conditions can distinguish underlying mechanisms according to their voltage dependence. The results also help to elucidate the mechanism of Ca^{2+} influx: the voltage dependence of I_{Ca} is bell-shaped, whereas Ca^{2+} influx through the Na^+–Ca^{2+} exchanger would increase exponentially at potentials more positive than −20 mV (heart ventricular myocytes: e.g. Barcenas-Ruiz, Beuckelmann & Wier, 1987; Barcenas-Ruiz & Wier, 1987; Kimura, Miyamae & Noma, 1987). In the present experiments, the voltage dependence of peak $[Ca^{2+}]_i$ was always bell shaped, supporting the idea that $[Ca^{2+}]_i$ is controlled by Ca^{2+} influx through Ca^{2+} channels, and the Ca^{2+} influx via the Na^+–Ca^{2+} exchanger is insignificant.

Recovery of $[Ca^{2+}]_i$ to resting values began immediately after Ca^{2+} influx was terminated by clamp steps to −50 mV. In the present study at 36 °C, the rate of recovery was about two times faster than that reported for 22 °C (Aaronson & Benham, 1989; Becker *et al.* 1989). The difference probably reflects the temperature sensitivity of active Ca^{2+} transport. Recovery is probably based on both the Ca^{2+}-ATPase of the sarcolemma and the Ca^{2+}-ATPase of the sarcoplasmic reticulum, the relative contribution of the two being unsettled. The rate of decay was insensitive to changes of the membrane potential between −50 and −100 mV, suggesting that Ca^{2+} extrusion through the sarcolemma cannot be due to electrogenic Na^+–Ca^{2+} exchange. The result also supports the view that Ca^{2+} extrusion from these smooth muscle cells is mostly due to an electroneutral Ca^{2+} pump.

During depolarizations lasting 10 s or longer, $[Ca^{2+}]_i$ rose within about 900 ms to a peak level (steps to 0 mV). This time course is similar to that observed in toad stomach (Becker *et al.* 1989), but shorter than in ureter (Aaronson & Benham, 1989). From the peak, $[Ca^{2+}]_i$ fell to a sustained level. For potentials between −40 and +80 mV, the sustained $[Ca^{2+}]_i$ was above resting $[Ca^{2+}]_i$; its bell-shaped voltage dependence seems to suggest a sustained Ca^{2+} influx through non-inactivated Ca^{2+} channels as the underlying mechanism (see below).

At steady state, the elevated $[Ca^{2+}]_i$ most probably stimulates the rate of Ca^{2+} extrusion (Ca^{2+}-ATPase) to equal the rate of Ca^{2+} influx. This might be possible if non-inactivated I_{Ca} is as small as several picoamperes (see e.g. Fig. 8*B*). Because the amplitude is so small, whole-cell measurements of non-inactivated I_{Ca} are difficult to perform (Imaizumi, Muraki, Takeda & Watanabe, 1989). Sustained Ca^{2+} influx through non-inactivated Ca^{2+} channels has been postulated for a long time. In multicellular preparations depolarized with excess potassium, sustained Ca^{2+} influx has been suggested by tonic (sustained) tension, sustained $^{45}Ca^{2+}$ influx, and by sustained elevation of $[Ca^{2+}]_i$ measured with aequorin (Morgan & Morgan, 1982) or

Fura-2 (Himpens & Somlyo, 1988). Recently, the patch-clamp technique has allowed Ca^{2+} influx through channels to be studied quantitatively. Sustained Ca^{2+} influx has been interpreted as I_{Ca} flowing in the potential window where steady-state activation and inactivation and curves overlap. 'Window I_{Ca}' should be maximal at about -20 mV (Klöckner & Isenberg, 1985*b*; Imaizumi *et al.* 1989; Lang, 1990). Direct measurements of non-inactivating I_{Ca} give controversial results. Studies of non-inactivating I_{Ca} by rapid application of calcium antagonists at constant potential showed maximal currents at -20 mV (Imaizumi *et al.* 1989); studies of non-inactivating I_{Ca} as a Ni^{2+}-sensitive difference current flowing at the end of 5 s pulses showed the same bell-shaped potential dependence as peak I_{Ca} (Aaronson, Bolton, Lang & MacKenzie, 1988). In the present experiments, I_{Ca} was not resolved at the level of a few picoamperes, and I_{Ca} was not defined as difference current. However, elevation of $[Ca^{2+}]_i$ induced by sustained depolarizations was consistently smaller at -20 mV than at 0 mV. Repolarizing ramp commands generated a bell-shaped voltage dependence for sustained level of $[Ca^{2+}]_i$ very similar to that of peak $[Ca^{2+}]_i$ and peak I_{Ca}. We extrapolate that the voltage dependence of non-activating I_{Ca} is similar to that of peak I_{Ca}. Thus, measurements of $[Ca^{2+}]_i$ under voltage clamp are useful for the interpretation of I_{Ca}. Similarly, depolarization-mediated changes in $[Ca^{2+}]_i$ can be used to separate the Ca^{2+} influx when it is superimposed by Cs^+ efflux through Ca^{2+} channels during clamp steps positive to the reversal potential of $+40$ mV (Fig. 4).

Inactivation of calcium channels (L-type) in various smooth muscle cells has been shown to be dependent on Ca^{2+} influx as well as on membrane potential. However, from our results the increase in $[Ca^{2+}]_i$ does not seem to be the immediate reason of inactivation since when $[Ca^{2+}]_i$ fell, inactivation remained (Fig. 5*A*). Also, the decay of $[Ca^{2+}]_i$ was not accelerated at more negative holding potentials although recovery of Ca^{2+} channels from inactivation occurs faster at more negative potentials (Ganitkevich, Shuba & Smirnov, 1987).

In vivo, smooth muscle cells of the urinary bladder, as well as most visceral smooth muscle cells, generate action potential spontaneously, and Ca^{2+} influx through voltage-operated Ca^{2+} channels might be regulated through the amplitude, duration, and frequency of the spikes. In addition, the cells generate slow depolarizations, due to stretch or under the influence of neurotransmitters or hormones. We have studied the effect of slow depolarizations on $[Ca^{2+}]_i$ with ramp commands that depolarized the membrane at slow rates. During very slow depolarizations, maximal increments in $[Ca^{2+}]_i$ were already reached at potentials as negative as -25 mV (Fig. 10 *C* and *D*). The interpretation of these results is difficult since one must account for time- and voltage-dependent gating (activation and inactivation) of Ca^{2+} channels. In addition, the Ca^{2+} channel is inactivated in a calcium-dependent manner. Interaction of all these mechanisms may be of special importance during agonist-mediated membrane depolarizations which can be accompanied by Ca^{2+} release from intracellular stores or by Ca^{2+} influx through non-selective cation channels.

We would like to thank Dr J. Picone for improving the manuscript.

REFERENCES

AARONSON, P. I. & BENHAM, C. D. (1989). Alterations in $[Ca^{2+}]_i$ mediated by sodium–calcium exchange in smooth muscle cells isolated from the guinea-pig ureter. *Journal of Physiology* **416**, 1–18.

AARONSON, P. I., BOLTON, T. B., LANG, R. J. & MACKENZIE, I. (1988). Calcium currents in single isolated smooth muscle cells from the rabbit ear artery in normal-calcium and high-barium solutions. *Journal of Physiology* **405**, 57–75.

ALMERS, W. & NEHER, E. (1985). The Ca signal from fura-2 loaded mast cells depends strongly on the method of dye loading. *FEBS Letters* **192**, 13–18.

BARCENAS-RUIZ, L., BEUCKELMANN, D. J. & WIER, W. G. (1987). Sodium–calcium exchange in heart: membrane currents and changes in $[Ca^{2+}]_i$. *Science* **238**, 1720–1722.

BARCENAS-RUIZ, L. & WIER, W. G. (1987). Voltage dependence of intracellular $[Ca^{2+}]_i$ transients in guinea-pig ventricular myocytes. *Circulation Research* **61**, 148–154.

BECKER, P. L., SINGER, J. J., WALSH, J. V. & FAY, F. S. (1989). Regulation of calcium concentration in voltage-clamped smooth muscle cells. *Science* **244**, 211–214.

BENHAM, C. D. (1989*a*). Voltage-gated and agonist-mediated rises in intracellular Ca^{2+} in rat clonal pituitary cells (GH_3) held under voltage clamp. *Journal of Physiology* **415**, 143–158.

BENHAM, C. D. (1989*b*). ATP-activated channels gate calcium entry in single smooth muscle cells dissociated from rabbit ear artery. *Journal of Physiology* **419**, 689–701.

BEUCKELMANN, D. J. & WIER, W. G. (1988). Mechanism of release of calcium from sarcoplasmic reticulum of guinea-pig cardiac cells. *Journal of Physiology* **405**, 233–255.

BOLTON, T. B. (1979). Mechanism of action of transmitters and other substances on smooth muscle. *Physiological Reviews* **59**, 606–718.

BOND, M., SHUMAN, H., SOMLYO, A. P. & SOMLYO, A. V. (1984). Total cytoplasmic calcium in relaxed and maximally contracted rabbit portal vein smooth muscle. *Journal of Physiology* **357**, 185–201.

CREED, K. E. (1971). Effects of ions and drugs on the smooth muscle cell membrane of the guinea-pig urinary bladder. *Pflügers Archiv* **326**, 127–141.

FABIATO, A. (1983). Calcium-induced release of calcium from the cardiac sarcoplasmic reticulum. *American Journal of Physiology* **245**, C1-14.

GANITKEVICH, V. YA., SHUBA, M. F. & SMIRNOV, S. V. (1987). Calcium-dependent inactivation of voltage-dependent calcium inward current in an isolated guinea-pig smooth muscle cell. *Journal of Physiology* **392**, 431–449.

GOLDMAN, W. F., WIER, W. G. & BLAUSTEIN, M. P. (1989). Effects of activation on distribution of Ca^{2+} in single arterial smooth muscle cells. Determination with Fura-2 and digital imaging microscopy. *Circulation Research* **64**, 1019–1029.

GRYNKIEWICZ, G., POENIE, M. & TSIEN, R. Y. (1985). A new generation of Ca^{2+} indicators with greatly improved fluorescence properties. *Journal of Biological Chemistry* **260**, 3440–3450.

HESS, P. & TSIEN, R. W. (1984). Mechanism of ion permeation through calcium channels. *Nature* **309**, 435–455.

HIMPENS, B. & SOMLYO, A. P. (1988). Free-calcium and force transients during depolarization and pharmacomechanical coupling in guinea-pig smooth muscle. *Journal of Physiology* **395**, 507–530.

IMAIZUMI, Y., MURAKI, K., TAKEDA, M. & WATANABE, M. (1989). Measurement and simulation of noninactivating Ca current in smooth muscle cells. *American Journal of Physiology* **256**, C880-885.

KIMURA, J., MIYAMAE, S. & NOMA, A. (1987). Identification of sodium–calcium exchange current in single ventricular cells if guinea-pig. *Journal of Physiology* **384**, 199–222.

KLÖCKNER, U. & ISENBERG, G. (1985*a*). Action potentials and net membrane currents of isolated smooth muscle cells (urinary bladder of the guinea-pig). *Pflügers Archiv* **405**, 329–339.

KLÖCKNER, U. & ISENBERG, G. (1985*b*). Calcium currents of caesium loaded isolated smooth muscle cells (urinary bladder of the guinea-pig). *Pflügers Archiv* **405**, 340–348.

LANG, R. J. (1990). The whole-cell Ca^{2+} channel current in single smooth muscle cells of the guinea-pig ureter. *Journal of Physiology* **423**, 453–473.

MELZER, W., SCHNEIDER, M. F., SIMON, B. J. & SZUCS, G. (1986). Intramembrane charge movement and calcium release in frog skeletal muscle. *Journal of Physiology* **373**, 481–511.

MORGAN, J. P. & MORGAN, K. G. (1982). Vascular smooth muscle: the first recorded Ca^{2+} transients. *Pflügers Archiv* **395**, 75–77.

NEHER, E. (1989). Combined fura-2 and patch clamp measurements in rat peritoneal mast cells. In *Neuromuscular Junction*, ed. SELLIN, L. C., LIBELIUS, R. & THESLEFF, S., pp. 65–76. Elsevier, Amsterdam.

SHUBA, M. F. (1981). The transport mechanisms by which contraction activating extracellular Ca ions enter smooth muscle cells. In *Molecular and Cellular Aspects of Muscle Function*, vol. 5, ed. VARGA, E., KÖVER, A., KOVAC, T. & KOVAC, L., pp. 83–94. Pergamon Press–Academiai Kaido, Budapest.

THAYER, S. A., HIRNING, L. D. & MILLER, R. J. (1988). The role of caffeine sensitive calcium stores in the regulation of the intracellular free calcium concentration in rat sympathetic neurones in vitro. *Molecular Pharmacology* **34**, 664–673.

YAGI, S., BECKER, P. L. & FAY, F. S. (1988). Relationship between force and Ca^{2+} concentration in smooth muscle as revealed by measurements on single cells. *Proceedings of the National Academy of Sciences of the USA* **85**, 4109–4113.

YAMAGUCHI, H. (1986). Recording of intracellular Ca^{2+} from smooth muscle cells by sub-micron tip, double-barrelled Ca^{2+}-selective microelectrodes. *Cell Calcium* **7**, 203–219.